Interference Functions, Pair Distribution Functions and Electron Transport Properties of Liquid Mercury-Indium Alloys *

N. C. HALDER † and C. N. J. WAGNER

Hammond Laboratory, Yale University, New Haven, Connecticut, USA

(Z. Naturforschg. **22 a**, 1489—1499 [1967]; received 2 May 1967)

X-ray diffraction patterns of liquid Hg–In alloys with 5, 12, 25, 35, 42, 50 and 62 atomic percent In were measured at room temperature (25 °C). The interference and radial distribution functions, $I(K)$ and $4\pi r^2 \varrho(r)$, respectively, were refined by an error analysis program. The position $K_1 = 4\pi \sin \Theta_1/\lambda$ of the first peak maximum of $I(K)$ does not change upon alloying, i. e., $K_1 = 2.29$ A^{-1}. The interference function of In plotted in reduced coordinates K/K_1 agrees with that calculated from the hard sphere model with a packing density of 45%. A small asymmetry of the first peak towards larger K values might be discernible in In, whereas the Hg and Hg–In interference functions show a relatively large asymmetry, and their subsequent peaks appear at larger K/K_1 values than those of the hard sphere model and In. The interatomic distances r_1 and the numbers of electrons η_E in the first coordination shell show only a small deviation from a linear relationship when plotted as a function of concentration.

Since $I(K)$ for $K < 2\,k_F$, where k_F is the FERMI radius, are rather similar for Hg, In and all measured alloys, the electrical resistivity and thermoelectric power were evaluated using the random model and ANIMALU and HEINE pseudopotentials. The predicted resistivity was found to increase from 30 $\mu\Omega$cm for pure Hg to 43 $\mu\Omega$cm for 35 atomic per cent In alloy and then to decrease to 24 $\mu\Omega$cm for pure In. The measured values of the resistivity decrease from 96 $\mu\Omega$cm for Hg to 30 $\mu\Omega$cm for pure In. Beyond the first eutectic composition, i. e., about 35 atomic per cent In concentration, the predicted resistivity curve decreases similarly to the measured resistivity curve. The discrepancy is attributed to the low density of states for Hg at the FERMI level. The predicted thermoelectric power decreases gradually from 1.22 μV/°K for pure Hg to 0.23 μV/°K for 62 atomic per cent In alloy, the value for pure In being 0.59 μV/°K. The measured values of thermoelectric power at 100 °C decrease first from −6.5 μV/°K for pure Hg to −7.1 μV/°K for 5 atomic per cent In alloy and then increase to −0.7 μV/°K for pure In. The discrepancy in the predicted values has been attributed to the energy dependence term of the pseudopotentials near the FERMI surface, particularly for pure Hg.

Of the mercury alloys, liquid Hg–Tl and Hg–In alloys have close resemblance in many respects, e.g., both are liquid at room temperature over considerable range of concentration, both look alike in the phase diagram [1, 2], and each of them has one intermediate phase of the average compositions Hg_5Tl_2 and Hg_5In_2, but Hg–In has an intermediate compound of composition HgIn. The measured resistivity-concentration curves [2, 3] of both the liquids show a negative deviation from a linear relationship. The HALL coefficients [2, 4], optical reflectivity [5], and compressibility [6] measurements of the two liquids also show similar variations with concentration.

The addition of trivalent In or Tl into Hg does not produce respective alloys of much different character although these two elements possess structural and electronic differences. There is a large difference between the atomic scattering powers of In and Tl, which fact produces a considerable LAUE monotonic scattering [7] (LMS) in Hg–In alloys and a negligible effect in Hg–Tl alloys. The structure of the former [8] could be explained with a fcc model while the latter [9] structure could be explained with a bcc model. The interatomic distances of liquid In (170 °C) and Tl (350 °C) are 3.18 and 3.30 Å respectively, and

† Present address: Department of Physics, State University of New York, Albany, New York.

* This investigation was supported by the United States Atomic Energy Commission.

[1] M. HANSEN, Constitution of Binary Alloys, McGraw-Hill Book Co., Inc., New York 1958, p. 842.
[2] N. E. CUSACK, P. KENDALL, and M. FIELDER, Phil. Mag. **10**, 871 [1964].
[3] A. ROLL and G. FEES, Z. Metallk. **51**, 1 [1960].
[4] A. A. ANDREEV and A. R. REGEL, Soviet Phys.-Solid State **7**, 2076 [1966].
[5] L. G. SCHULZ, Advanc. Physics **6**, 102 [1957].
[6] R. B. GORDON, Trans. Met. Soc. AIME **227**, 51 [1963].
[7] N. C. HALDER and C. N. J. WAGNER, Tech. Rept. No. 9, June 1966, United States Atomic Energy Commission, AT (30-1) 2560.
[8] H. OCKEN and C. N. J. WAGNER, Phys. Rev. **149**, 122 [1966].
[9] N. C. HALDER and C. N. J. WAGNER, J. Chem. Phys. **45**, 482 [1966].

each element has about eleven atoms within the first coordination sphere. The DIRAC–SLATER (DS) atomic scattering powers of In do not agree as closely as those of Tl and Hg with those observed from x-ray interference function and radial distribution function (RDF). The agreement between the measured and predicted values of the resistivities is worse in liquid In [8] than in liquid Tl [9]. Also the predicted values of the thermoelectric power for liquid In was not as good as those observed in liquid Tl. However, the agreement between the predicted and measured values of the resistivity and thermoelectric power was worst in liquid Hg.

Thus, a dissimilar character of the liquids In and Tl but a similar nature of their alloys Hg–In and Hg–Tl suggest a worthwhile x-ray investigation of these two liquid alloys. We have earlier studied liquid Hg–Tl [10] alloys using x-ray diffraction technique and tried to resolve some of the questions like the formation of molecular grouping in the compound composition Hg_5Tl_2, the diffuseness of the peak intensity of the alloy of the first eutectic composition (Hg–8.5 Tl) and whether the free electron model could be applicable to this alloy. Our conclusions were that all the Hg–Tl alloys could be described by a close packed fcc model and there was no evidence for molecular grouping in liquid Hg_5Tl_2 alloy. Besides, an evaluation of the resistivity and thermoelectric power using theoretical model potentials and the substitutional model of FABER and ZIMAN [11] indicated that the disagreement was quite serious for the dilute Hg alloys. This could be a consequence of the Hg pseudopotentials which influence the dilute alloys more strongly in this region than Tl. This effect was found to be destroyed beyond the first eutectic composition. In a recent paper MOTT [12] has suggested that the very low density of states at the FERMI surface, which is lower than the free electron value in Hg, must involve a correction factor in the original ZIMAN [13] theory for liquid metals. Similar effects have been also predicted in liquid Ca, Sr and Ba. Incorporating MOTT's idea into ZIMAN's equation, the situation can be improved, i.e., the predicted resistivity of liquid Hg may be increased from 30 to 60 $\mu\Omega$cm and the nature of both the predicted and experimental resistivity-concentration plot can be made to look alike. Still the predicted values of the resistivity of Hg and its alloys fall much below the experimental values (for Hg the experimental value of the resistivity is 96 $\mu\Omega$cm).

Presently, we shall describe an investigation on liquid Hg–In alloys using x-ray diffraction technique and attempt to see if results similar to the ones found in Hg–Tl are obtained. The atomic distribution functions will be used for structural information and the free electron model theory will be applied for an evaluation of the transport properties. The results will be compared with the available experimental values.

I. Experimental

Hg–In alloys of compositions 5, 12, 25, 35, 42, 50 and 62 atomic per cent In were prepared using triply distilled Hg and 99.999% pure In. Chances of oxidation were prevented by using a dry box and 80 per cent helium and 20 per cent hydrogen gas mixture. The alloy specimens and pure Hg were studied at room temperature 25 °C in a plexiglass sample holder, whereas pure In was heated to 170 °C in a pyrolytic graphite boat [8]. The experimental arrangements for the alloys were similar to that of the Hg–Tl systems [10]. The high temperature setups have been described in our earlier publications [8, 9, 14]. The diffracted intensities were measured on a theta-theta diffractometer with monochromatized MoK_α radiation between $2\vartheta = 8°$ and 130°. An interval of 0.25° in 2ϑ was selected for scattering between 8° and 30° and it was increased to 0.50° in 2ϑ between 30° and 130°. Every time pure Hg and tungsten powder were used to check the diffractometer alignment and stability of the incident beam.

The corrections of the background, COMPTON and LAUE monotonic scattering were applied. The absorption and polarization effects were corrected and then the measured intensity was converted to electron units, i.e., $I_{eu}^{coh}(K)$, where $K = 4\pi \sin\vartheta/\lambda$. The high angle (HA) and RDF method of normalization procedures were followed. A detailed account of the error analysis and normalization procedure is available elsewhere [7].

[10] N. C. HALDER, R. J. METZGER, and C. N. J. WAGNER, J. Chem. Phys. **45**, 1259 [1966].
[11] T. E. FABER and J. M. ZIMAN, Phil. Mag. **11**, 153 [1965].
[12] N. F. MOTT, Phil. Mag. **13**, 989 [1966].
[13] J. M. ZIMAN, Phil. Mag. **6**, 1013 [1961].
[14] C. N. J. WAGNER, H. OCKEN, and M. L. JOSHI, Z. Naturforschg. **20 a**, 325 [1965].

II. Results

A. Measured Intensity

The intensity of the coherent scattering in electron units (eu) from a binary alloy can be writen[10] as:

$$I_{\text{eu}}^{\text{coh}}(K) = \langle f^2 \rangle + \langle f \rangle^2 \int_0^\infty 4\pi r^2 [\varrho(r) - \varrho_0] \frac{\sin K r}{(K r)} \, \mathrm{d}r \tag{1}$$

where $\langle f^2 \rangle = \sum_{i=1}^{2} c_i f_i^2$ and $\langle f \rangle^2 = \sum_{i=1}^{2} (c_i f_i)^2$.

ϱ_0 is the average density and $\varrho(r)$ represents the radial density or the pair distribution function. c_i and f_i are respectively the atomic concentration and atomic scattering factors of the elements. The interference functions defined by

$$I(K) = [{}_{\text{eu}}^{\text{coh}}(K) - \langle f^2 \rangle + \langle f \rangle^2] / \langle f \rangle^2 = 1 + \int_0^\infty 4\pi r^2 [\varrho(r) - \varrho_0] \frac{\sin K r}{(K r)} \, \mathrm{d}r \tag{2}$$

were calculated. This function was then used to determine the RDF:

$$4\pi r^2 \varrho(r) = 4\pi r^2 \varrho_0 + \frac{2r}{\pi} \int_0^\infty K[I(K) - 1] \sin K r \, \mathrm{d}K . \tag{3}$$

B. Pair Distribution and Interference Function

The radial density function $\varrho(r)$ is given by

$$\varrho(r) = [\sum_{i=1}^{2} \sum_{j=1}^{2} c_i f_i f_j \varrho_{ij}(r)] / \langle f \rangle^2 \tag{4}$$

where $\varrho_{ij}(r)$ is the number of atoms of type j per unit volume at a distance r from an atom of type i. It is easily seen that

$$\varrho_i(r) = \sum_{j=1}^{2} \varrho_{ij}(r) \qquad \text{and} \qquad c_i \varrho_{ij}(r) = c_j \varrho_{ji}(r) . \tag{5}$$

Therefore, the radial density $\varrho(r)$ can be written as:

$$\varrho(r) = [c_1 f_1^2 \varrho_1(r) + c_2 f_2^2 \varrho_2(r) - c_1 (f_1 - f_2)^2 \varrho_{12}(r)] / (c_1 f_1 + c_2 f_2)^2 . \tag{6}$$

The coherently scattered radiation ${}_{\text{eu}}^{\text{coh}}(K)$ [Eq. (1)] can be obtained in terms of the partial interference function[15] $I_{ij}(K)$:

$$I_{\text{eu}}^{\text{coh}}(K) = c_1 c_2 (f_1 - f_2)^2 + \sum_{i=1}^{2} \sum_{j=1}^{2} c_i c_j f_i f_j I_{ij}(K) \tag{7}$$

where $$I_{ij}(K) = 1 + \int_0^\infty 4\pi r^2 \left[\frac{\varrho_{ij}(r)}{c_j} - \varrho_0 \right] \frac{\sin K r}{K r} \, \mathrm{d}r = I_{ji}(K) . \tag{8}$$

Using Eqs. (5) we can also write

$$I_{\text{eu}}^{\text{coh}}(K) = c_1 c_2 (f_1 - f_2)^2 + c_1 f_1^2 I_1(K) + c_2 f_2^2 I_2(K) - c_1 c_2 (f_1 - f_2)^2 I_{12}(K) \tag{9}$$

where $$I_i(K) = \sum_{j=i}^{2} c_i I_{ij}(K) = 1 + \int_0^\infty 4\pi r^2 [\varrho_i(r) - \varrho_0] \frac{\sin K r}{K r} \, \mathrm{d}r . \tag{10}$$

The refined interference function plots [Eq. (2)] are shown in Fig. 1. These were refined through the function $G(r) = 4\pi r[\varrho(r) - \varrho_0]$ which are plotted in Fig. 2. The refinement procedure has been discussed in our earlier papers [8, 9]. The peak maximum positions of the interference functions were determined from the enlarged refined plots, and are

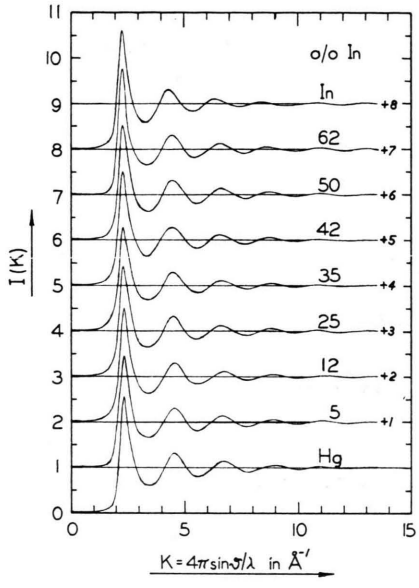

Fig. 1. The plots of interference functions $I(K)$ for liquid Hg–In alloys measured at room temperature, except pure In which was measured at 170 °C.

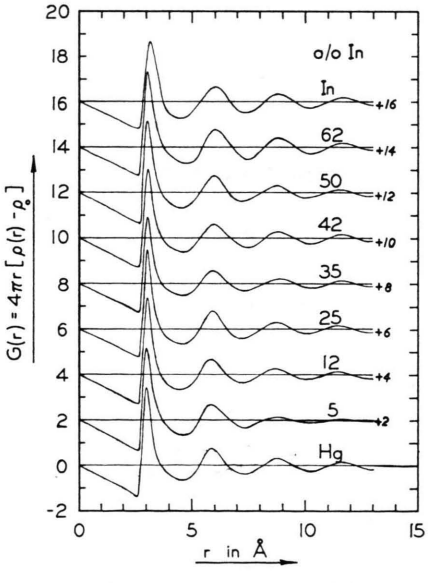

Fig. 2. The plots of $G(r) = 4\pi r[\varrho(r) - \varrho_0]$ for liquid Hg–In alloys measured at room temperature, except pure In which was measured at 170 °C.

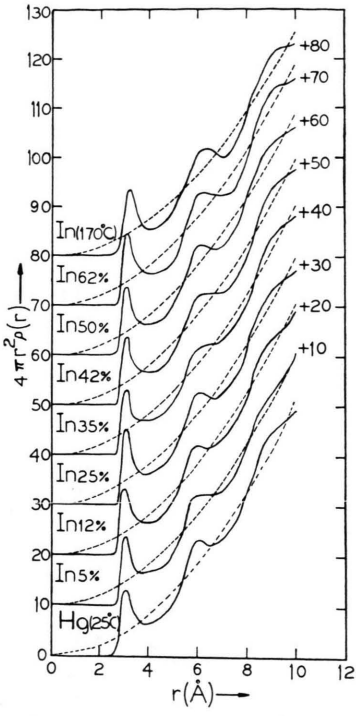

Fig. 3. The plots of radial distribution functions $4\pi r^2 \varrho(r)$ for liquid Hg–In alloys. The dashed lines represent the uniform distributions $4\pi r^2 \varrho_0$.

Composition at % In	K_1 Å^{-1}	K_2 Å^{-1}
0	2.29	4.54
5	2.29	4.54
12	2.29	4.55
25	2.29	4.50
35	2.29	4.50
42	2.29	4.50
50	2.29	4.44
62	2.29	4.43
100	2.29	4.29

Table 1. Peak maximum positions of the interference function $I(K)$ for liquid Hg–In alloys.

given in Table 1. The interatomic distances r_1 obtained from the RDF plots [Fig. 3] and pair probability function $P(r) = \varrho(r)/\varrho_0$ are shown in Table 2. The macroscopically measured [16] values of ϱ_0 of the alloys were employed.

C. Coordination Numbers and Number of Electrons in the First Coordination Shell

The coordination number was calculated with the equation

$$\eta = \int_{r_0}^{r_2} 4\pi r^2 \varrho(r)\, dr . \qquad (11)$$

Composition at % In	ϱ_0 atoms Å^{-3}	r_1[RDF] Å	r_1[$P(r)$] Å	r_0 Å	r_2 Å	η atoms
0	0.0407	3.05	3.02	2.00	3.82	10.0
5	0.0405	3.05	3.02	2.00	3.84	10.1
12	0.0404	3.04	3.00	2.00	3.88	10.2
25	0.0401	3.07	3.05	2.00	3.90	10.3
35	0.0398	3.08	3.06	2.00	3.95	10.3
42	0.0396	3.09	3.07	2.00	4.00	10.9
50	0.0393	3.09	3.07	2.00	4.00	11.0
62	0.0389	3.11	3.09	2.00	4.08	11.0
100	0.0368	3.18	3.12	2.00	4.14	11.0

Table 2. Interatomic distances r_1 and coordination numbers η obtained with $K_{max}=15.6$ Å^{-1} for liquid Hg–In alloys.

The values of r_0, r_2 and η are given in Table 2. The total number of electrons in the first coordination shell was calculated from

$$\eta_E = \langle Z\rangle \eta , \tag{12}$$

where

$$\langle Z\rangle = \sum_i c_i Z_i .$$

Z_i is the atomic number of the element i. η_E can also be expressed [17] as

$$\eta_E = \langle Z\rangle \eta_R + \Delta\eta_E , \tag{13}$$

where η_R is the coordination number in a random solution. The quantity $\Delta\eta_E$ represents a deviation from the linearity of the plot η_E versus c. The η_E–c plot is shown in Fig. 4.

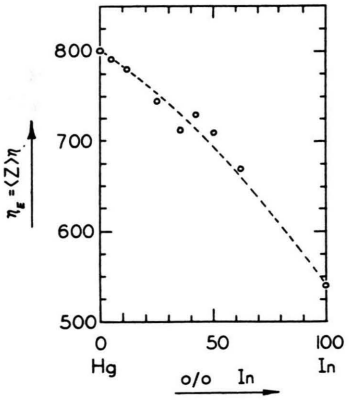

Fig. 4. The plot of total number of electrons η_E in the first coordination shell for liquid Hg–In alloys.

D. Electron Transport Properties

The electrical resistivity and thermoelectric power were evaluated with the refined interference functions and Animalu and Heine [18] pseudopotentials. For calculation of resistivity and thermoelectric power the Faber and Ziman [11] equation for the random model was used. The justification for using this model will be discussed in the next section. However we will give here the basic equations that lead to the determination of the resistivity and thermoelectric power.

If it is possible to study an alloy whose atoms are distributed in a random way, we will have

$$\varrho_i(r) = \varrho_{ij}(r)/c_j = \varrho^R(r). \tag{14}$$

Similarly the interference functions will yield:

$$I_i(K) = I_{ij}(K) = I(K). \tag{15}$$

Eqs. (14) and (15) greatly simplify the form of the equation representing the scattering cross section as a function of the pseudopotential elements of the solute and solvent ions. The general equation for the scattering cross section, i. e.,

$$|V(K)|^2 = \langle U^2\rangle - \langle U\rangle^2 + \sum_{i=1}^{2}\sum_{j=1}^{2} c_i c_j U_i(K) U_j(K) I_{ij}(K),$$

reduces to

$$|V(K)|^2 = c_1 c_2 [U_1(K) - U_2(K)]^2 [1 - I(K)] + [c_1 |U_1(K)|^2 + c_2 |U_2(K)|^2] I(K), \tag{16}$$

where $U_i(K)$ is the matrix element of the pseudopotential of element i. Then the resistivity ϱ_R and thermoelectric power Q can be computed from

$$\varrho_R = [3\pi (m^*)^2/(e^2 \hbar^3 k_F^2 \varrho_0)] \langle |V(K)|^2\rangle \tag{17}$$

and

$$Q = [\pi^2 k^2 T/(3 e E_F)] \cdot [3 - 2|V(2k_F)|^2/\langle |V(K)|^2\rangle], \tag{18}$$

[15] C. N. J. Wagner and N. C. Halder, Conference on the Properties of Liquid Metals, September 19–23, 1966, Brookhaven National Laboratory, Upton, New York; Advan. Phys., in press.

[16] D. A. Olsen and D. C. Johnson, J. Phys. Chem. **67**, 2529 [1963].

[17] S. Steeb and R. Hezel, Z. Phys. **191**, 398 [1966].

[18] A. O. E. Animalu and V. Heine, Phil. Mag. **12**, 120 [1965].

Composition at % In	$2k_F$ Å^{-1}	Predicted ϱ_R μΩcm	Predicted Q μV/°K	Experimental ϱ_R μΩcm	Experimental Q μV/°K
0	2.68	29.87	1.22	95.8	−6.5
5	2.70	35.56	0.40	80.3	−7.1
12	2.73	37.01	0.28	66.0	−5.5
25	2.77	39.99	−0.22	51.8	−3.5
35	2.81	43.25	−0.41	46.2	−2.6
42	2.83	37.98	−0.10	43.5	−2.2
50	2.86	36.48	−0.11	40.8	−1.7
62	2.89	30.35	0.23	37.4	−1.3
100	—	—	—	30.0	−0.7
100 (M.P.)	2.97	24.30	0.59	32.5 [a]	−1.0 [b]

a S. Takeuchi and H. Endo, Trans. Japan. Inst. Metals **3**, 30 [1962]. b A. S. Marwaha and N. E. Cusack, Phys. Letters **22**, 556 [1966].

Table 3. Fermi diameter $2k_F$, resistivity ϱ_R and thermoelectric power Q for liquid Hg–In alloys. The experimental values are those reported by Cusack et al. [2] and are read from their figures. Note that the experimental Q values are referring to temperature 100 °C. The values for indium at the melting point are taken from references [a] and [b].

where

$$\langle |V(K)|^2 \rangle = 4 \int_0^1 |V(K)|^2 (K/2k_F)^3 \, d(K/2k_F). \quad (19)$$

The symbols k and T respectively represent the Boltzmann constant and the absolute temperature. The Fermi radius k_F is given by $k_F = (3\pi^2 z \varrho_0)^{1/3}$, where z is the valence, and $E_F = \hbar^2 k_F^2/(2m^*)$ is the Fermi energy. The predicted values of the resistivity and thermoelectric power are shown with the experimental values of Cusack et al. [2] in Table 3.

In the above equations, $U_i(K)$ is related to the pseudopotential element $U_i^{AH}(K)$ calculated by Animalu and Heine [18], i. e.,

$$U_i(K) = (\varrho_0/\varrho_i^0) U_i^{AH}(K),$$

where $\varrho_0 = \sum_i c_i \varrho_i^0$ is the average atomic density of the alloy and ϱ_i^0 is the average atomic density of element i. With the above definition of $U_i(K)$, the quantity ϱ_0 will remain in the denominator of Eq. (17). If one chooses the value of the $U_i(K)$ per atom instead of per unit volume as calculated by Animalu and Heine [18], i. e.,

$$[U_i(K)] = U_i^{AH}(K)/\varrho_i^0,$$

the average atomic density ϱ_0 will appear in the numerator of Eq. (17). Another point we wish to mention is that the values $U_i(K)$ are usually given as a function of $K/2k_F$ where k_F is the Fermi radius of element i. In the alloys it is necessary to know the pseudopotential elements $U_i(K)$ to a value of $(2k_F)_{\text{Alloy}}$ which might be larger than $(2k_F)_{\text{Element}}$ of type i.

III. Discussion

A. Interference Function

Since the measurements for all liquid alloys were made at 25 °C, except for In, all our discussion should refer to a study of their structures at temperatures which are 45 to 65 °C above the liquidus temperature. A temperature variation of 20 °C should be unimportant to produce any significant structural change in the liquid alloys [9].

The position K_1 of the first peak maximum in the interference function $I(K)$ does not change upon alloying In into Hg, i. e., $K_1 = 2.29$ Å^{-1}. Only a small variation can be observed in the position K_2 of the second peak maximum. In Hg–Tl alloys, K_1 was found to change slightly from 2.29 Å^{-1} for Hg to 2.26 Å^{-1} for Tl. The exact determination of K_1 has been of considerable importance because of its strong influence on the value of the predicted electron transport properties. As mentioned above, the position K_1 and the height $I(K_1)$ of the first Hg peak maximum were used for repeated checks of the alignment of the diffractometer [8].

Liquid In can be reasonably well described [8] by the hard sphere (HS) model using a packing density $d = \pi \varrho_0 D^3/6 = 0.45$. This leads to a hard sphere diameter of $D = 2.86$ Å. As the density of closest packing in solids is $d_c = 0.74$, it is easy to see that $d_c/d = 1.65$ which agrees with the value calculated by Furukawa [19] from a quasi-face-centered cubic lattice model of liquids. The reduced interference function $I(K')$ is plotted in Fig. 5 as a function of $K' = K/K_1$, where K_1 is the position of the first peak maximum, for hard spheres [20] with $d = 0.45$, and

for liquid In. There seems to be a slight asymmetry in the first peak of In when compared with the HS model, liquid Ag or Tl which are also shown in Fig. 5.

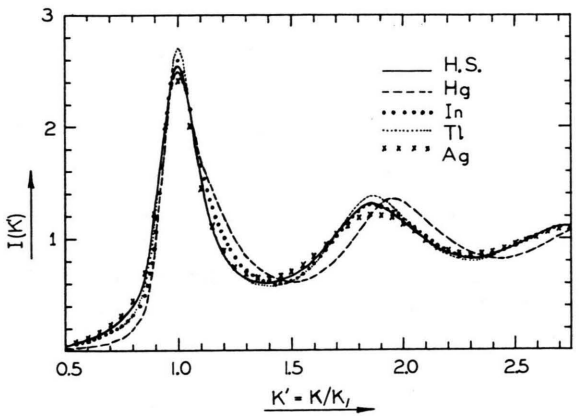

Fig. 5. The plots of interference functions $I(K')$ in reduced coordinate $K'=K/K_1$ for liquid Hg (25 °C), Tl (350 °C), In (170 °C), and Ag (1050 °C). The hard sphere model interference function obtained with packing density 0.45 is also shown. Note the agreement between all except liquid Hg whose first peak is asymmetric as compared to others and the second peak maximum is shifted to a larger value of K'.

Liquid Hg, however, shows a large asymmetry of the first peak, also described as a shoulder [21], when compared with HS of packing density $d=0.45$ or Ag. This has been interpreted as a consequence of the presence of β-Hg structure above the melting point in the predominantly α-Hg-like liquid [21]. Part of the asymmetry of Hg, when compared with Ag, or Au as done by RIVLIN et al. [21], is due to the fact that the second peak occurs at larger values of $K'=K/K_1$ than that of the close packed liquid Ag. As shown by KAPLOW et al. [22] when comparing atomic distribution functions with a quasi-fcc or hcp model, liquid Hg does not fit such a close packed model. This deviation has been interpreted by HEINE and WEAIRE [23] as a consequence of the proximity of the position $K_0=2.39$ Å^{-1} where the first zero of the pseudopotential matrix elements occurs, and the value of $K_1=2.29$ Å^{-1} of the first peak maximum of the interference function of Hg. A similar but smaller effect should also be observed in In where $K_0=2.47$ Å^{-1} and $K_1=2.29$ Å^{-1}, and, as mentioned above, a slight asymmetry might be discernible in the first peak of $I(K)$.

B. Atomic Distribution Functions

The $G(r)$ and RDF plots (Figs. 2 and 3) do not show any structure other than the pure liquids. Indeed, the reduced distribution functions $G(r)$ of pure Hg and pure In are rather similar, only the positions of the first and second peaks are at slightly higher values in liquid In. Therefore, one does not expect drastic changes in the alloys. The broadening of the peaks in the RDF curves are found to increase gradually. As shown in Fig. 6

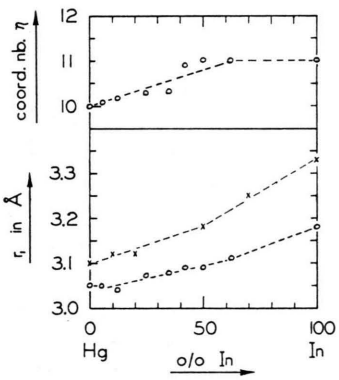

Fig. 6. The plots of interatomic distance r_1 and coordination number η for liquid Hg–In alloys. ⊙: present investigation, ×: KIM et al. [24].

the weighted interatomic distances r_1 increase linearly from 3.05 Å for Hg to 3.11 Å for 62 atomic per cent In alloy. The value of r_1 for pure In measured [8] at 170 °C was found to be 3.18 Å. The r_1 vs. concentration plot shows a slight negative deviation from a linear relationship (VEGARD's law), which is a consequence of the heavy weight of the Hg atoms in the radial density $\varrho(r)$. In Hg – Tl alloys a positive deviation from VEGARD's law was found [10]. Somewhat larger values of r_1 were obtained by KIM et al. [24] in an earlier study on Hg–In alloys. We believe that this was the result of a large damping factor $\exp(-\gamma K^2)$ applied to the measured interference function $I(K)$ in order to reduce the weight of $I(K)$ at large values of K in the FOURIER transformation. This effect is similar to the reduction of

[19] K. FURUKAWA, Sci. Rept. Res. Inst. Tohoku Univ. Ser. A **12**, 368 [1960].
[20] N. W. ASHCROFT and J. LEKNER, Phys. Rev. **145**, 82 [1966].
[21] V. G. RIVLIN, R. M. WAGHORNE, and G. I. WILLIAMS, Phil. Mag. **13**, 1169 [1966].
[22] R. KAPLOW, S. L. STRONG, and B. L. AVERBACH, Phys. Rev. **138**, A 1336 [1965].
[23] V. HEINE and D. WEAIRE, Phys. Rev. **152**, 603 [1966].
[24] Y. S. KIM, C. L. STANDLEY, R. F. KRUH, and G. T. CLAYTON, J. Chem. Phys. **34**, 1464 [1961].

the limit of integration K_{max} which also increases the values of r_1 [14].

The coordination number η increases from 10 atoms in Hg to 11 atoms in pure In. The number of electrons η_E in the first coordination shell decreases almost linearly with increasing In concentration (Fig. 4), which indicates that Hg–In alloys are rather random solutions [17].

No anomalies were observed either in the case of the 12 atomic per cent In or 50 atomic per cent In alloys which are the intermediate phases. The β-phase ($\sim$12 per cent In) is believed to be tetragonal [25], whereas the compound HgIn is said to be ordered, but its structure has not yet been established.

The molar heat of mixing of Hg–In alloys is negative, but rather small, reaching a minimum value of -540 cal/g atom at 50 atomic per cent In. This indicates that Hg–In alloys tend to be rather random solutions. This supports the fact that η_E deviates little from a linear law when plotted as a function of concentration. Kim et al. [24] calculated the shapes of the first peak in the RDF for the alloys assuming a random superposition of the pair Hg–Hg, Hg–In and In–In centered at 3.15, 3.22 and 3.30 Å respectively, which agreed well with their observed curves.

C. Change of Resistivity with Concentration

The electrical resistivity of the liquid alloys has been evaluated with the measured interference function $I(K)$ and the theoretically calculated potential elements assuming that the alloys are random solutions, i. e., $I_i(K) = I_{ij}(K) = I(K)$. If the weighted interference functions do not show any observable change upon alloying between $0 < K < 2k_F$, in particular if the positions and heights of the first peak maximum do not change, it is reasonable to assume that $I_1(K)$, $I_2(K)$ and $I_{12}(K)$ are approximately equal below $2k_F$. This condition was fulfilled in the Hg–In alloys, i. e., in these alloys the change in resistivity was mostly due to the change in $2k_F$ with concentration.

All that we have said above is equivalent to using the equation for the substitutional model, which has been described by Faber and Ziman [11]. It may be pointed out however that the use of the substitutional model, as it is, has some additional requirements, i.e., the atomic volumes of the two components should be equal, the replacement of a solvent ion by a solute ion should occur without creating a change in the scattering and the dilatation effect of the solvent by a solute atom is negligible. It seems therefore probable that the random model is a good approximation below $2k_F$ for evaluating the transport properties of liquid Hg–In alloys.

The predicted and experimentally measured values of the resistivities are shown in Fig. 7. The solid line represents the experimental curve due to Cusack et al. [2] and the circles indicate our predicted points. It is obvious that the predicted points do not reproduce the experimental trend of the plot. The

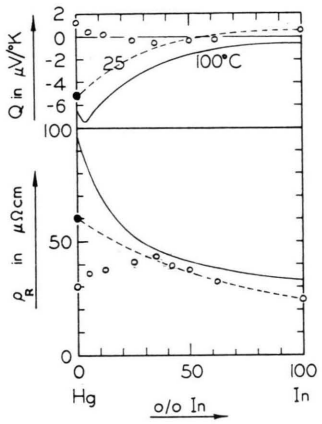

Fig. 7. The plots of electrical resistivity ϱ_R and thermoelectric power Q for liquid Hg–In alloys. The solid lines denote the experimental plot after Cusack et al. [2], and the open circles are the predicted points. The points denoted by solid circles are obtained after applying Mott's [12] correction factor for ϱ_R and Bradley et al.'s [34] correction factor for Q.

predicted resistivities are smaller and increase first from 30 $\mu\Omega$cm for pure Hg to 43 $\mu\Omega$cm for 35 atomic per cent In alloy. Beyond this point the predicted values are comparatively less far off the experimental curve, and the shape of both the curves is almost similar. Indeed, for Hg–Tl alloys similar results were obtained. Remarkably, in each of the alloys the predicted shapes agree well with the experimental ones right after the first eutectic composition.

The disagreement in the dilute Hg alloys originates with the Hg structure. It has been of great interest [12, 23] recently to solve the problem of Hg based on its various experimental results which can not otherwise be explained with the general ap-

[25] B. R. Coles, M. F. Merriam, and Z. Fisk, J. Less-Common Metals 5, 41 [1963].

proach followed in other divalent metals like Zn. The very low melting point of Hg has been considered to be an indication of a different type of electronic structure in Hg from other group II metals. MOTT [12] suggested that the density of states near the FERMI level in Hg falls below the free electron value. This idea of MOTT introduces a correction factor g^{-2} in the original ZIMAN equation [11]. Therefore, the equation for resistivity now becomes:

$$(\varrho_R)_{cor} = g^{-2}(\varrho_R)_{Ziman}$$

where g is the ratio between the two density of states, i. e., $g = N(E_F)/[N(E_F)]_{\text{Free Electron}}$. The value of g is speculative rather than experimental For liquid Hg we find that the corrected value of resistivity is 60 $\mu\Omega$cm if we assume $g^{-2} = 2$. Even then the disagreement does not disappear. Now supposing that the disagreement in pure In was for a reason other than the low density of states, as in Hg, we can explain the resistivity-concentration plot between pure Hg and 35 atomic per cent In alloy. Using $g^{-2} = 2$ for Hg, let us say $g^{-2} = 1$ for 35 atomic per cent In alloy and make a linear interpolation between these two points against concentration. This will then give us g^{-2} values for all the points between Hg and 35 atomic per cent In alloy. Indeed, with these interpolated values of g^{-2} we will get points which will be close to the smooth curve passing through the Hg point. The corrected values are given in Table 4. The predicted curve then looks

Composition at % In	g^{-2}	q'	Corrected ϱ_R $\mu\Omega$cm	Corrected Q μV/°K
0	2.00	−10.0	59.6	−5.11
5	1.86	− 8.5	66.14	−4.06
12	1.68	− 6.5	62.17	−3.13
25	1.36	− 2.8	54.39	−1.70

Table 4. Corrected resistivity obtained with MOTT's [12] g factor and corrected thermoelectric power obtained with BRADLEY et al.'s [34] q' factor. For the alloys the correction factors were obtained by interpolation.

reasonable and the scattering of the points falls within the limits of the error bars. In so doing, it has been invariably assumed that the influence of the low density of states of Hg persists as far as 35 atomic per cent In alloy, a physical justification of which follows later. When we extend our calculation to Hg–Tl alloys with 8.5 atomic per cent Tl as the limiting boundary the predicted curve nicely represents the trend of the experimental curve. However, the differences in magnitude may be interpreted as a consequence of the inadequacy of the pseudopotential elements. This point has been discussed by SPRINGER [26], WISER [27] and HEINE and WEAIRE [23].

Let us now turn our attention to the point where the density of states of the alloys becomes approximately equal to that of a free electron liquid. BRADLEY [28] has measured the pressure dependence of resistivity and thermoelectric power for liquid Hg–In alloys and noted that the effect of alloying and increasing the pressure on the density of states will tend to decrease the minimum of $N(E)$ versus E plot [Fig. 1 of ref. [28]] and g will approach unity. With alloying he found that the density of states becomes free electron like above about 20 atomic per cent In. The measurements of spin paramagnetic susceptibility [29, 30] of Hg–In alloys indicate that the PAULI-LANDAU susceptibility agrees with the free electron theory beyond 35 atomic per cent In. It is believed [29] that the deviation in the dilute alloys and pure Hg can be understood from the low density of states of Hg near the FERMI level. The change in KNIGHT shift, i. e., $\Delta S/S$ has been measured by SEYMOUR and STYLES [31] as a function of concentration for the In resonance in liquid Hg–In alloys. In the above $S = 8\pi/3\,\Omega\,\chi_p\,P_F$ is the shift with $\Omega =$ atomic volume, $\chi_p =$ electron spin susceptibility per unit volume and $P_F =$ average probability density at the nucleus for electron at the FERMI level. The behavior of their $\Delta S/S$-concentration curve for Hg–In alloys shows a deviation from the free electron model. However, the experimental curve agrees reasonably well with the calculated curve when using the observed PAULI-LANDAU susceptibilities, as shown by GÜNTHERODT et al. [29]. BUSCH and GÜNTHERODT [32] argued that the FERMI radius could

[26] B. SPRINGER, Phys. Rev. **136**, A 115 [1964].
[27] N. WISER, Phys. Rev. **143**, 393 [1966].
[28] C. C. BRADLEY, Phil. Mag. **14**, 953 [1966].
[29] H. J. GÜNTHERODT, A. MENTH, and Y. TIÈCHE, Phys. kondens. Materie **5**, 392 [1966].
[30] E. W. COLLINGS, Conference on the Properties of Liquid Metals, September 19—23, 1966, Brookhaven National Laboratory, Upton, New York; Advan. Phys., in press.
[31] E. F. W. SEYMOUR and G. A. STYLES, Proc. Phys. Soc. London **87**, 473 [1966].
[32] G. BUSCH and H. J. GÜNTHERODT, Conference on the Properties of Liquid Metals, September 19—23, 1966, Brookhaven National Laboratory, Upton, New York; Advan. Phys., in press.

be defined by

$$k_F = [3\pi^2/(e R_H)]^{1/3},$$

where R_H is the experimental value of the HALL coefficients which might deviate from the free electron value. However, more accurate values of the density data could explain [32] the observed discrepancy between the experimental HALL coefficients in Hg–In and Hg–Tl alloys and the free electron values. ANDREEV and REGEL [4] measured the HALL coefficients for liquid Hg–Tl alloys and concluded that in liquid Hg–Tl as well as in Hg–In alloys the density fluctuation of the scale of short range order produce favorable conditions for the appearance of a higher valence in heavy metal atoms. This is equivalent to saying a higher k_F should be used and coincides with the interpretation of BUSCH and GÜNTHERODT [32]. From these arguments we reasonably believe that the density of states of the alloys becomes approximately equal to that of the corresponding free electron liquid after about 30 atomic per cent In.

D. Thermoelectric Power

The experimentally measured value of the thermoelectric power Q for Hg at 25 °C is $-5\,\mu V/°K$ whereas our predicted value is $1.22\,\mu V/°K$. Disagreement similar to this has been reported by SUNDSTRÖM [33] whose value was $1.38\,\mu V/°K$.

In calculating the pseudopotentials it was assumed [18] that $U(K)$ was independent of the state vector k. This assumption may not be too serious as far as the calculations of the resistivities are concerned, but an evaluation of the thermoelectric power has been found to be strongly affected by it. BRADLEY et al. [34] pointed out that the pseudopotential for Hg depend upon the energy near the FERMI surface. In other words, the matrix elements linking the incident and scattered wave should depend upon the angle of the scattering, i. e., K as well as k. Allowing for this k dependence correction of the pseudopotential, we get:

$$x = 3 - 2q - q'/2\,, \tag{20}$$

where $$q = |V(2k_F)|^2/\langle |V(K)|^2\rangle$$

and

$$q' = k_F \langle (\partial |U(K)|^2/\partial k) I(K)\rangle/\langle |U(K)|^2 I(K)\rangle.$$

A value $q' = -10$ was postulated by BRADLEY et al. [34] but the later work of SUNDSTRÖM [33] states $q' = -1.2$. There is a difficulty in using the latter value of q'; first, because it does not eliminate the observed disagreement and secondly, it postulates the existence of a virtual bound state near the FERMI energy, which is rather unlikely. In the absence of any numerical value of the dependence of $U(K)$ on k, although the problem has been theoretically treated by ANIMALU and HEINE [18], we shall use $q' = -10$ for Hg and correct our predicted values. The plot obtained with the corrected Hg point for Q values are shown in Fig. 7. Assuming again that the anomalous effect of Hg is affecting the first three points and allowing for their corrections from a linear interpolation, it can be shown that the agreement is reasonably good. The explanation we wish to offer regarding the absence of the small peak [2] near 5 atomic per cent In is the difference of temperature. From the experimental curves it is evident that the peak becomes sharper with higher temperature. Similar effects have been observed in Hg–Tl alloys [15]. The quantity q does depend on temperature and consequently q'. Most of the contribution to q for a change of temperature comes from $I(K)$ rather than $U(K)$. An alternative explanation of the small peak present in the experimental curve has been offered by MOTT [12] and later by BRADLEY [28] in his recent paper. He argued that because Q is proportional to $(d\sigma/dE)_{E=E_F}$, where σ is the electrical conductivity, it should depend on the slope of the density of states curve $(dN(E)/dE)_{E=E_F}$. For small concentration the quantity x [Eq. (20)] increases before g becomes sufficiently large in order to make the dip more shallow.

IV. Conclusions

The results of the investigations on liquid Hg–In alloys show that the weighted interatomic distances and the weighted coordination numbers of the alloys are dominated by the more strongly scattering Hg atoms. This then gives rise to a negative deviation from a linear law to be obtained with the points corresponding to the pure elements. The interference functions of the alloys look similar and

[33] L. J. SUNDSTRÖM, Phil. Mag. **11**, 657 [1966].

[34] C. C. BRADLEY, T. E. FABER, E. G. WILSON, and J. M. ZIMAN, Phil. Mag. **7**, 865 [1962].

the positions of the first peak maximum do not seem to change upon alloying. This fact along with the thermodynamical data, namely the heat of mixing, the change in entropy, and the linear behavior of the density, leads us to conclude that the three partial interference functions which characterize the scattering are approximately equal, at least below $K = 2\,k_F$. Therefore one can reasonably assume that the theory of FABER and ZIMAN [11] developed for dilute alloys, should also be applicable to Hg–In alloys. The predicted resistivity plot agrees qualitatively well with the experimental plot if a correction factor for the low density of states for Hg near the FERMI level is used. The change of the resistivity in Hg–In alloys is mostly due to the change in $2\,k_F$ and the concentration. The predicted values of the thermoelectric powers for Hg and the dilute alloys agree with the experimental values if the contribution of the energy dependence term of the pseudopotentials for Hg near the FERMI level is considered. The results of magnetic susceptibility and HALL coefficients, which ordinarily do not agree with the values obtained from free electron approximation, may be explained qualitatively well if the MOTT [12] corrected density of states for Hg, similar to that applied for the electrical resistivity, is used.

Thermodynamische Untersuchung diffusionsloser Phasenumwandlungen im System Gold–Cadmium

BRUNO PREDEL und WERNER SCHWERMANN

Institut für Metallforschung der Universität Münster (Westf.)

(Z. Naturforschg. **22 a**, 1499—1503 [1967]; eingegangen am 29. Juni 1967)

Im System Gold–Cadmium wurde die Energetik der diffusionslosen Umwandlungen $\beta_1 - \beta'$ (bei 47,5 Atom-% Cd) und $\beta_1 - \beta''$ (bei 49 Atom-% Cd) untersucht. Mit Hilfe eines empfindlichen Kleinkalorimeters gelang eine direkte Bestimmung der Umwandlungsenthalpien und eine Festlegung des Temperaturbereiches, innerhalb dessen die jeweilige Reaktion vollständig abläuft. Die Ergebnisse dieser thermischen Untersuchungen ermöglichten nach elektronenmikroskopischer Bestimmung der Zwillingslamellendicke in den Martensitphasen eine Ermittlung der Zwillingsgrenzflächenenergie für die Phasen β' und β''. Ferner wurde der Einfluß eindimensionaler und hydrostatischer Druckbelastungen auf die Verschiebung des Martensitpunktes diskutiert.

Bei den meisten bisher durchgeführten Untersuchungen diffusionsloser Phasenumwandlungen in metallischen Systemen stand die Klärung der kristallographischen Verhältnisse im Vordergrund des Interesses. Durch Ermittlung der speziellen strukturellen Eigenheiten und insbesondere durch eine genaue Bestimmung der Orientierungszusammenhänge zwischen Ausgangs- und Endphase konnten verschiedentlich die Umwandlungsmechanismen erschlossen werden. Eine unmittelbare Untersuchung der Energetik diffusionsloser Phasenumwandlungen, die in manchen Fällen wertvolle Aufschlüsse liefern kann, ist indessen, zum Teil bedingt durch experimentelle Schwierigkeiten, nur in sehr geringem Umfang erfolgt.

Für den Ablauf einer diffusionslosen Phasenänderung ist in energetischer Hinsicht die Bilanz zwischen dem Gewinn an freier Umwandlungsenthalpie und dem Aufwand an freier Enthalpie für energieverzehrende, mit der Strukturänderung zwangsläufig gekoppelte Nebenreaktionen ausschlaggebend. In der Regel wird die freie Umwandlungsenthalpie bei der Entstehung von Phasengrenzflächen, Stapelfehlern oder elastischen Gitterverzerrungen verbraucht.

Durch Ausbildung kristallographischer Zwillinge in der martensitischen Phase kann in geeigneten Systemen die Gitterverzerrungsenergie reduziert werden. Das ist z. B. bei den Umwandlungen der β_1-Phase im System Gold–Cadmium der Fall. Unter anderem hat das zur Folge, daß die Phasenumwandlungen innerhalb eines engen Temperaturintervalls vollständig zu Ende laufen. Damit ist die Möglichkeit gegeben, mit einem geeigneten kalorimetrischen Verfahren die gesamte Umwandlungsenthalpie unmittelbar während des Reaktionsablaufes zu bestimmen und unter Berücksichtigung der speziellen thermischen und kristallographischen Gegebenheiten einen direkten Einblick in die energetischen Verhältnisse des Umwandlungsprozesses zu gewinnen.